sciendo
Polish Journal of Medical Physics and Engineering
The Journal of Polish Society of Medical Physics
ISSN 1898-0309, doi: 10.2478/pjmpe-2020-0008
June 2020
Vol 26, Issue 2

Scientific Paper

A numerical study on the effect of conductivity change in cell kill distribution in irreversible electroporation

Amir KHORASANI[1,a]
[1]*Department of Medical Physics, School of Medical Sciences, Isfahan University of Medical Science, Isfahan, Iran*
[a]*E-mail address: amir69k@yahoo.com*

(received 30 January 2020; accepted 4 May 2020)

Abstract

Introduction: irreversible electroporation (IRE) is a tissue ablation technique and physical process used to kill the undesirable cells. In the IRE process by mathematical modelling we can calculate the cell kill probability and distribution inside the tissue. The purpose of the study is to determine the influence of electric conductivity change in the IRE process into the cell kill probability and distribution.

Methods: cell death probability and electric conductivity were calculated with COMSOL Multiphysics software package. 8 pulses with a frequency of 1 Hz, pulse width of 100 μs and electric field intensity from 1000 to 3000 V/Cm with steps of 500 V/Cm used as electric pulses.

Results: significantly, the electrical conductivity of tissue will increase during the time of pulse delivery. According to our results, electrical conductivity increased with an electric field intensity of pulses. By considering the effect of conductivity change on cell kill probability, the cell kill probability and distribution will change.

Conclusion: we believe that considering the impact of electric conductivity change on the cell kill probability will improve the accuracy of treatment outcome in the clinic for treatment with IRE.

Key words: electroporation; Finite Element Analysis; electric conductivity; Peleg-Fermi; pulsed electric field.

Introduction

During electroporation, cells are exposed to the sufficiently high voltage electric field pulses that increase the transmembrane potential (TMP) of the cell membrane above a threshold [1-3]. The result of this increase in TMP is pore formation in the cell membrane. If the cell membrane recovers and pores were closed, reversible electroporation (RE) occurred. In the RE the cells remain viable. Reversible electroporation is used to transfer of macromolecules into the cells [4]. The combination of RE and chemotherapeutic agents has been used for cancer treatment which named electrochemotherapy (ECT) [5].

But if the cell membrane cannot recover and permanent pores were formed, irreversible electroporation (IRE) has occurred and the consequent is cell dies [6-9]. Recently, IRE with minimally invasive ablation and without joule heating effects is used for the treatment of tumors [10,11]. The IRE is used as a unique mode of cell death that does not rely on thermal damage from joule heating [8,12-14].

Successful IRE therapy depends on treatment planning parameters such as electric field intensity, frequency of the pulses, number of pulses and electrical tissue parameters, etc. Inducing maximum damage to the tumor and minimum damage to the surrounding healthy tissue is one of the most important parameters. This parameter is accomplished by numerical models. Several numerical models describing cell kill probability as a function of the electric field intensity [15,16]. These models are usually based on experimental data. The Peleg-Fermi model as a mathematical model is the most usable model for expression of cell death during IRE [17-19]. The Peleg-Fermi model in comparison with other models seems the most adequate because it includes dependency of pulse number and electric field intensity. For this reason, in this study Peleg-Fermi model was used.

The goal of IRE is inducing the cell death of undesirable cells. There are some factors that affect cell kill probability. One of the most important factors is electric field magnitude and distribution inside the tissue [20]. The electric field distribution and magnitude depends on the electric pulse and tissue properties and electrodes configuration [21]. Electrical conductivity is one of the tissue properties which can affect the electric field distribution and magnitude. Different studies have shown an increase in tissue conductivity in IRE [22-24]. The goal of this study was to describe the effects of electrical conductivity change during IRE on the cell kill distribution.

Material and methods

Finite element and parameter model

To calculate a finite element model, COMSOL Multiphysics 5.3 finite element analysis software was used. A cube geometry with dimensions 32*32*17 mm was modeled as liver tissue. A pair of stainless-steel needle electrodes with 0.43 mm diameter was used for simulation. The distance between the two electrodes is 8.66 mm. **Figure 1** represented the electrodes and tissue geometries that were used in this study. In this study, a triangular meshing model which contained 56194 mesh nodes were used. The geometry was created in symmetric model, in order to reduce the simulation time (**Figure 1**).

8 pulses with a frequency of 1 Hz, pulse width of 100 µs and electric field intensity from 1000 to 3000 V/Cm with steps of 500 V/Cm used as electric pulses. The electrical and thermal properties of the liver and electrodes are listed in **Table 1** [25,26].

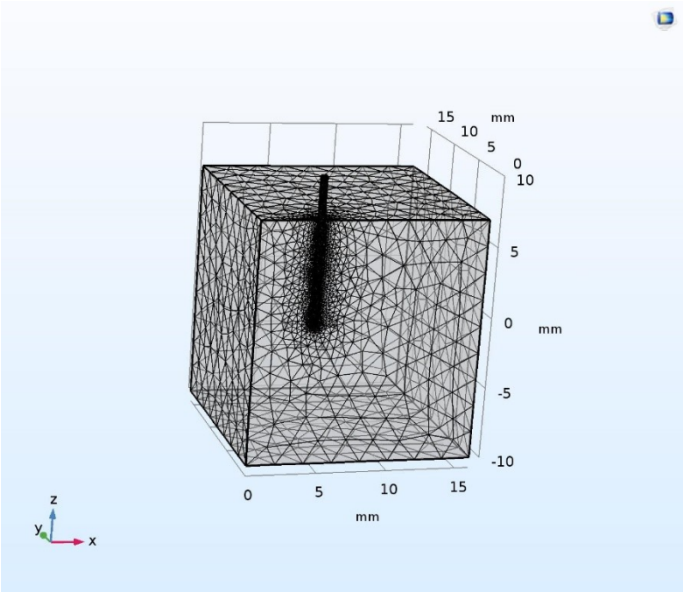

Figure 1. Geometry of numerical modeling and meshing the model

Calculating method

The electric field and electric potential distribution inside the tissue were obtained by Laplace's equation:

$$\vec{\nabla}.\left(\sigma.\vec{\nabla}\varphi\right) = 0 \qquad \text{Eq. 1}$$

Where σ and φ are tissue conductivity and electrical potential, respectively. Heat transfer in the tissue was estimated using Penne's Bioheat equation:

$$\nabla.(k\nabla T) + \sigma|\nabla\varphi|^2 + q''' - W_b c_b T = \rho c_p \frac{\partial T}{\partial t} \qquad \text{Eq. 2}$$

where T is temperature, φ is electrical potential, q‴ is the heat produced by metabolism, $W_b c_b T$ is the heat produced by perfusion, ρ is density, and c_p is specific heat capacity of the tissue. The conductivity changes in the IRE inside the tissue was calculated as [25,26]:

$$\sigma = \sigma_0 \cdot (1 + \text{flc2hs}(E - E_{delta}, E_{range}) + \alpha \cdot (T - T_0)) \qquad \text{Eq. 3}$$

where σ_0 is tissue initial conductivity, E is the electric field in the deserted point, E_{delta} is threshold electric field in electroporation, E_{range} is electric field range, α is temperature coefficient, T is the temperature of the tissue, and T_0 is the initial temperature of the tissue. Additionally, flc2hs is a smoothed Heaviside function in the COMSOL that changes from zero to one when $E - E_{delta} = 0$ over the range E_{range} to ensure the convergence of the numerical solution [25]. The parameters used in **Equation 3**, are listed in **Table 2**.

The electrical boundary condition at the active row of electrodes was set to be $\varphi = V(t)$. Where V(t) were pulses with time-varying voltage. Another row of electrodes was set at$\varphi = 0$. The remaining boundaries were considered as electrical insulation.

Table 1. The electric and thermal properties of the liver and stainless-steel electrodes

	Electrical conductivity (S/m)	Thermal conductivity (W/m.K)	Density (kg/m^3)	Heat capacity (J/kg.K)	reference
electrode	1.398*10^6	16.3	7800	490	[25,26]
liver	0.067 (initial)	0.512	1050	360	[25,26]

Table 2. Parameters used in the simulation

Variables	Variable values	reference
σ_0	0.067 (S/m)	[25,26]
E_{delta}	580 (V/cm)	[25,26]
E_{anger}	(120, -120) (V/cm)	[25,26]
α	0.015 (°C^{-1})	[25,26]
T_0	37 (°C)	[25,26]

The mathematical model used to calculate the cell kill due to IRE. The Peleg-Fermi model is given by:

$$S(E,N) = \frac{N}{N_0} = \frac{1}{1+e^{\left(\frac{E-E_c(N)}{A(N)}\right)}} \qquad \text{Eq. 4}$$

where S is the ratio of surviving cells, N is the number of surviving cells after IRE treatment, N_0 is the number of cells prior to IRE treatment, E is an electric field, $E_c(N)$ is the critical electric field in which 50% of the cells are killed, and A(N) is a function of the pulse number. This model accounts for dependency on the number of pulses and electric field during IRE. In equation $E_c(N)$ and A(N) is given by:

$$E_c(N) = E_0 e^{-k_1 n} \qquad \text{Eq. 5}$$

$$A(N) = A_0 e^{k_2 n} \qquad \text{Eq. 6}$$

where $E_0 = 399{,}600\ V/m$, $A_0 = 144{,}100\ V/m$, $k_1 = 0.03$ and $k_2 = 0.06$ [17].

These equations resulted from fit the experimental data to **Equation 4** which performed by Globerg et al. [17]. Additionally, because we wanted to calculate the percentage cell kill, we converted the cell viability into a percentage cell kill given by:

$$P_{kill} = 100(1 - S) \quad \text{Eq. 7}$$

Results

The results of this work are divided into two parts: conductivity change during IRE and percentage cell kill during IRE treatment.

Conductivity change during IRE

In this work, the conductivity changes were calculated in two points, tip and middle of electrodes. The conductivity changes of 8 pulses with 2500 V/cm electric field intensity during pulse transmission time are presented in **Figure 2**. When the intensity of the electric field was higher than the critical value, an increase in conductivity has occurred. As we can see in **Figure 2**, tissue conductivity in the transmission time of pulses was increased. This increase in the tip of the electrode was higher than in between electrodes. The conductivity changes at the time of last pulses (8^{th}) with different electric field intensity are listed in **Table 3**.

Percentage cell kill during IRE treatment

To investigate the impact of conductivity change during IRE on the cell kill distribution two groups of simulations were done. One group of simulations is done with constant conductivity and other groups are done with variable conductivity which is given by **Equation 3**.

I have presented the cell kill probability histogram with different pulses in **Figure 3**. The cell kill probability histogram represents the frequency of occurrence of cell kill probability which lies within a volume fraction of simulated tissue. The cell kill probability histogram for 3000 V/cm pulses with variable and constant tissue electrical conductivity during IRE are shown in **Figure 4**.

We can use two-dimensional and three-dimensional images for a better showing of the percentage cell kill distribution inside the tissue. **Figures 5** and **6** display the percentage cell kill distribution due to IRE around the electrode for different pulse electric field intensity. The percentage cell kill distribution in **Figures 5** and **6** are calculated with variable and constant electrical conductivity during the IRE respectively. In order to visualize the percentage of cell kill due to IRE in 3D, the volume of the liver which has a cell kill probability of more than 80% are presented in **Figures 7** and **8** for different pulses. Simulation results in **Figures 7** and **8** are calculated with variable and constant electrical conductivity respectively.

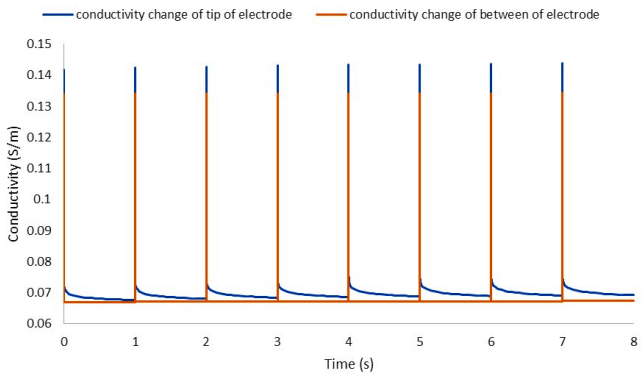

Figure 2. Conductivity changes used 8 pulses with the frequency of 1 Hz, pulse width of 100 µs, and the intensity of the electric fields of 2500 V/cm in the tip and between of electrode

Table 3. Conductivity change in the tip and between the electrodes at the time of the last pulse with 8 pulses with the frequency of 1 Hz, pulse width of 100µs, and electric field intensity of 1000-3000 V/cm

Electric field intensity (V/cm)	Tip (S/m)	Between (S/m)
1000	0.136	0.134
1500	0.139	0.134
2000	0.143	0.134
2500	0.149	0.134
3000	0.157	0.134

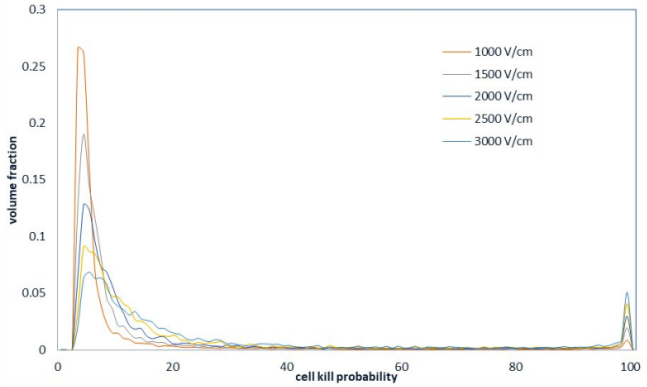

Figure 3. Cell kill probability histogram at last pulse (8th) for 1000-1500-2000-2500-3000 V/cm electric field intensity of pulses with variable electrical conductivity during IRE

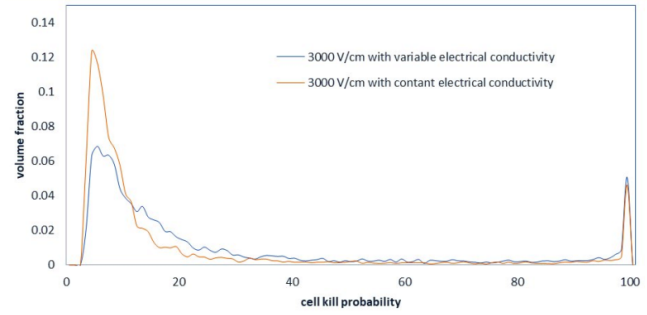

Figure 4. The cell kill probability histogram at last pulse (8th) for 3000 V/cm pulses with variable and constant tissue electrical conductivity during IRE

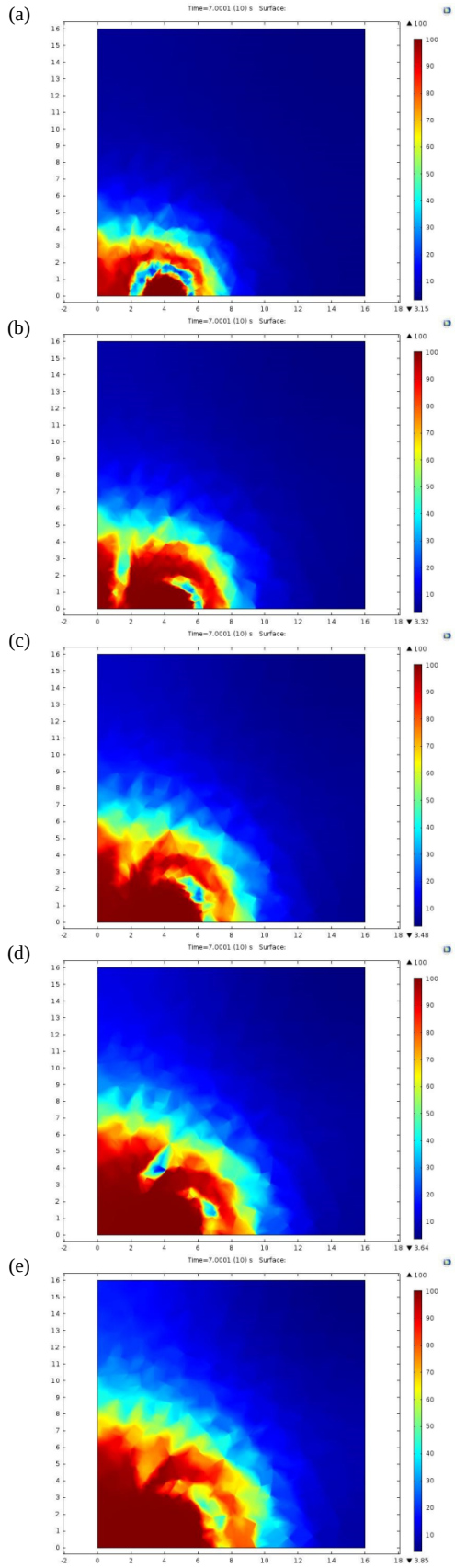

Figure 5. The percentage cell kill distribution due to IRE around the electrode in the plane perpendicular to the tip of electrodes at last pulse (8th) with variable electric conductivity for pulses with a) 1000 V/cm b) 1500 V/cm c) 2000 V/cm d) 2500 V/cm e) 3000 V/cm electric field intensity.

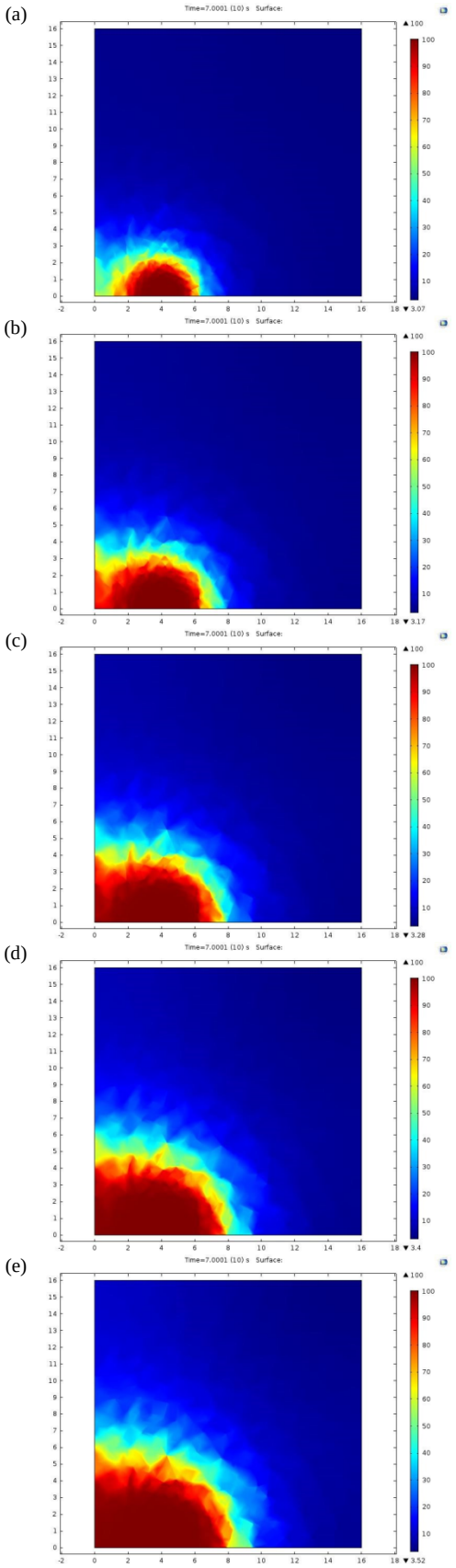

Figure 6. The percentage cell kill distribution due to IRE around the electrode in the plane perpendicular to the tip of electrodes at last pulse (8th) with constant electric conductivity for pulses with a) 1000 V/cm b) 1500 V/cm c) 2000 V/cm d) 2500 V/cm e) 3000 V/cm electric field intensity.

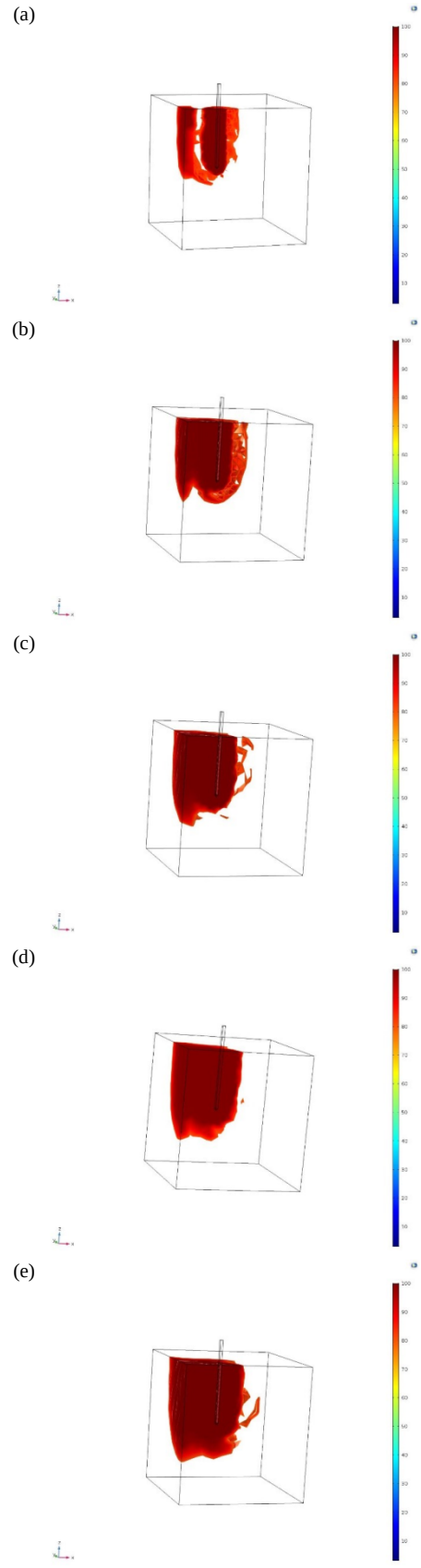

Figure 7. Volume of the liver which has a cell kill probability of more than 80% at last pulse (8th) with variable electric conductivity for pulses with a) 1000 V/cm b) 1500 V/cm c) 2000 V/cm d) 2500 V/cm e) 3000 V/cm electric field intensity.

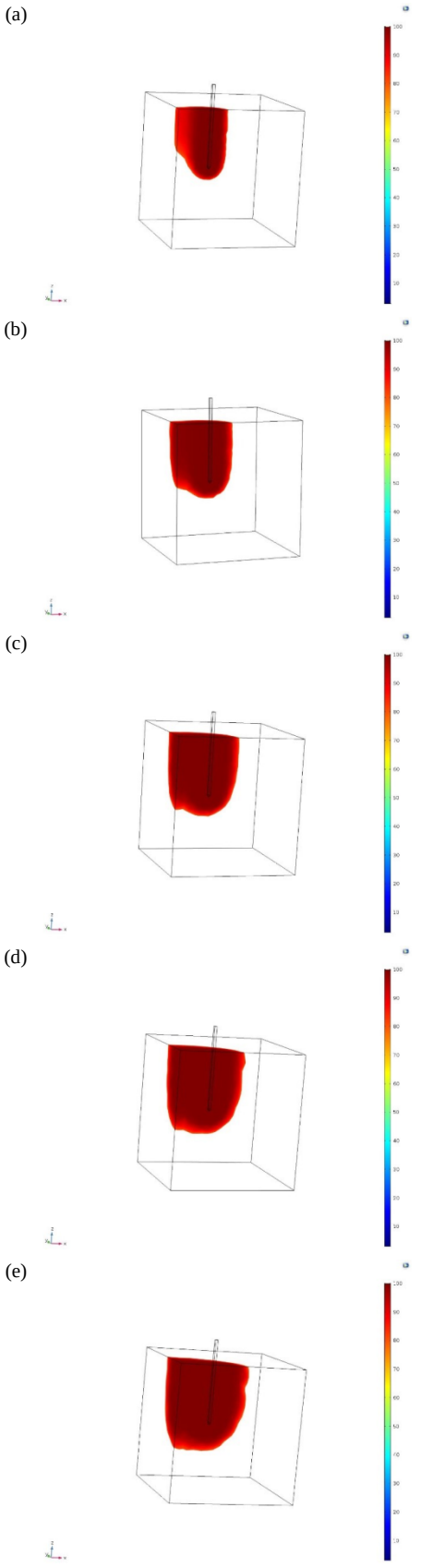

Figure 8. Volume of the liver which has a cell kill probability of more than 80% at last pulse (8th) with constant electric conductivity for pulses with a) 1000 V/cm b) 1500 V/cm c) 2000 V/cm d) 2500 V/cm e) 3000 V/cm electric field intensity.

In order to better visualize the volume fraction of tissue killed by IRE, **Figure 9** was calculated. **Figure 9** displays the computed volume fraction of tissue which has cell kill probability of more than 80% as a function of the electric field intensity of electric pulses. Figure 9 provides the calculated volumes of tissue killed with constant and variable tissue electrical conductivity during the simulation.

Discussion

IRE is a new and invasive ablation technique with nonthermal effects. In order to visualized the cell kill probability distribution and maximizing damage to the tumor and minimizing damage to the surrounding healthy tissue, numerical models have been developed [27-30].

According to the Peleg-Fermi equation (**Equation** 4) some factors affecting the cell kill distribution such as electric field intensity, number of pulses, etc. Tissue electrical conductivity is one of the factors which can affect the electric field intensity inside the tissue and therefore can change cell kill probability. In this study, initially, the tissue electric conductivity change was calculated during the IRE for different pulses (**Figure 2**, **Table 3**). The remarkable result to emerge from the data is that the tissue electrical conductivity increased with an electric field intensity of pulses. This is in good agreement with [31,32]. The observed increase in tissue electrical conductivity could be attributed to being a result of pore creation in the cell membrane during pulse delivery. Which pore creation increased with an electric field intensity of pulses (**Table 3**). As expected, simulation results demonstrate that the change of tissue electrical conductivity because of greater electric field intensity in the tip of the electrode is more than in point of between electrodes. This confirms our previous findings [31,33].

As stated in the introduction, the main goal of this work was to describe the effects of different electric field intensity and tissue electrical conductivity change during IRE on the cell kill probability distribution.

Figures 5 and **6** are showing the cell kill probability distribution for different pulses. It is important to note that the cell kill probability increased with the electric field intensity of pulses. Importantly, cell kill probability is higher in the vicinity of electrodes because of greater electric field intensity in this region. This finding highlights the usefulness of greater electric filed intensity of pulses for the treatment of big tumors. A reasonable explanation for this phenomenon is that, with an increase of electric field intensity of the pulse, the volume of tissue which has cell kill probability >80% become bigger, and high electric field intensity pulses can use for bigger tumor. These findings correlate fairly well with [17].

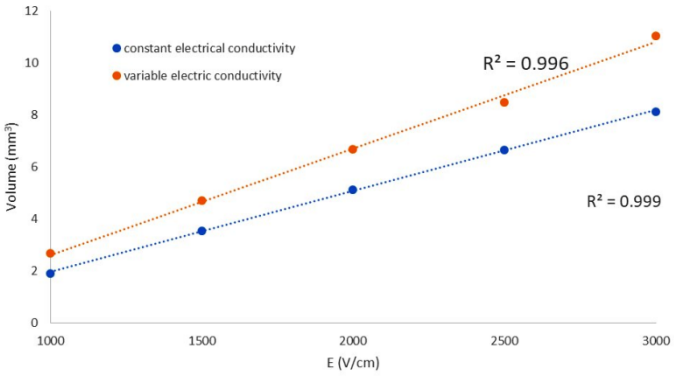

Figure 9. Volume of tissue that has cell kill probability of more than 80% as a function of the electric field intensity of electric pulses with constant and variable electrical conductivity.

Histogram (**Figures 3** and **4**) analysis showed that, with an increase of electric field intensity of pulses, the volume fraction of tissue with low cell kill probability was reduced and volume fraction of tissue with high cell kill probability was increased. These results offer powerful evidence for tumor treatment with an adequate electric field intensity of pulses. The experiment in this work is in line with previous results [34,35]. **Figure 4** is representing the cell kill probability histogram for 3000 V/cm pulses with constant and variable tissue electric conductivity. According to the results, it is important to note that with variable tissue electric conductivity during IRE, the volume fraction of tissue with low cell kill probability was reduced and the volume of tissue with high cell kill probability was increased in constant electric field intensity of pulse. These results match well with **Figure 4**. The possible reasons for this result are, during the transmission time of pulse, the pore was created in the cell membrane. The result of pore creation is an increase in the electric conductivity of the medium. The consequence of tissue electric conductivity raise is an increase in electric current and electric field intensity in the far region of the electrode. According to the Peleg-Fermi equation (**Equation 4**) the cell kill probability is related to the electric field intensity. So because of an increase in electric field intensity in the far region of the electrode, the cell kill probability was increased. And change the cell kill probability distribution inside the tissue (**Figures 5-8**).

Conclusion

One of the goals of treatment planning in IRE is identification the treated volume of target tissue before the IRE process being started. The key to successful treatment is ensuring that the tumor treated with sufficient cell kill probability during the treatment. This is done by numerical models such as finite element methods. This paper has evaluated the importance of electric conductivity change and electric field intensity of pulse on cell kill probability. The results of this paper have demonstrated that, by considering the impact of electric conductivity change on cell kill probability, the cell kill

probability was changed. So, in order to accurate prediction of treatment in treatment planning, it has been suggested to considering the role of electric conductivity change on cell kill probability. The results have obtained satisfactory demonstrating that for treatment of the big tumor, we can use pulses with high electric field intensity. However, using the pulses with high electric field intensity increase the temperature of tissue [36] and must be considered. This is important for future research to survey the impact of electrical conductivity change on tissue temperature raise during IRE.

References

[1] Weaver JC. Electroporation: a general phenomenon for manipulating cells and tissues. Journal of Cellular Biochemistry. 1993;51(4):426-435.

[2] Weaver JC, Chizmadzhev YA. Theory of electroporation: a review. Bioelectrochemistry and Bioenergetics. 1996;41(2):135-160.

[3] Kotnik T, Kramar P, Pucihar G, et al. Cell membrane electroporation-Part 1: The phenomenon. IEEE Electrical Insulation Magazine. 2012;28(5):14-23.

[4] Weaver JC. Electroporation of cells and tissues. IEEE Transactions on Plasma Science. 2000;28(1):24-33.

[5] Edhemovic I, Brecelj E, Gasljevic G, et al. Intraoperative electrochemotherapy of colorectal liver metastases. Journal of Surgical Oncology. 2014;110(3):320-327.

[6] Appelbaum L, Ben-David E, Sosna J, et al. US findings after irreversible electroporation ablation: radiologic-pathologic correlation. Radiology. 2012;262(1):117-125.

[7] Ben-David E, Appelbaum L, Sosna J, et al. Characterization of irreversible electroporation ablation in in vivo porcine liver. American Journal of Roentgenology. 2012;198(1):W62-W68.

[8] Rubinsky B. Irreversible electroporation in medicine. Technology in Cancer Research & Treatment. 2007;6:255-259.

[9] Lu DS, Kee ST, Lee W. Irreversible electroporation: ready for prime time? Techniques in Vascular and Interventional Radiology. 2013;16(4):277-286.

[10] Rubinsky B, Onik G, Mikus P. Irreversible electroporation: a new ablation modality—clinical implications. Technology in Cancer Research & Treatment. 2007;6:37-48.

[11] Onik G, Mikus P, Rubinsky B. Irreversible electroporation: implications for prostate ablation. Technology in Cancer Research & Treatment. 2007;6:295-300.

[12] Chu KF, Dupuy DE. Thermal ablation of tumours: biological mechanisms and advances in therapy. Nature Reviews Cancer. 2014;14(3):199-208.

[13] Ahmed M, Brace CL, Lee Jr FT, Goldberg SN. Principles of and advances in percutaneous ablation. Radiology. 2011;258(2):351-369.

[14] Garcia PA, Rossmeisl JH, Neal RE, et al. A parametric study delineating irreversible electroporation from thermal damage based on a minimally invasive intracranial procedure. Biomedical Engineering Online. 2011;10;34.

[15] Huang K, Tian H, Gai L, Wang J. A review of kinetic models for inactivating microorganisms and enzymes by pulsed electric field processing. Journal of Food Engineering. 2012;111(2):191-207.

[16] Peleg. Advanced quantitative microbiology for foods and biosystems: models for predicting growth and inactivation: CRC Press, 2006.

[17] Golberg A, Rubinsky B. A statistical model for multidimensional irreversible electroporation cell death in tissue. Biomedical Engineering Online. 2010;9:13.

[18] Dermol J, Miklavcic D. Predicting electroporation of cells in an inhomogeneous electric field based on mathematical modeling and experimental CHO-cell permeabilization to propidium iodide determination. Bioelectrochemistry. 2014;100:52-61.

[19] Garcia PA, Davalos RV, Miklavcic C. A numerical investigation of the electric and thermal cell kill distributions in electroporation-based therapies in tissue. PLoS One. 2014;9:e103083.

[20] Miklavcic D, Corovic S, Pucihar G, Pavselj N. Importance of tumour coverage by sufficiently high local electric field for effective electrochemotherapy. European Journal of Cancer Supplements. 2006;4(11):45-51.

[21] Adeyanju OO, Al-Angari HM, Sahakian AV. The optimization of needle electrode number and placement for irreversible electroporation of hepatocellular carcinoma. Radiol Oncol. 2012;46(2):126-35.

[22] Dunki-Jacobs EM, Philips P, Martin 2nd RC. Evaluation of resistance as a measure of successful tumor ablation during irreversible electroporation of the pancreas. J Am Coll Surg. 2014;218(2):179-87.

[23] Moisescu MG, Radu M, Kovacs E, et al. Changes of cell electrical parameters induced by electroporation. A dielectrophoresis study. Biochim Biophys Acta. 2013;1828:365-72.

[24] Kranjc M, Bajd F, Sersa I, Miklavcic D. Magnetic resonance electrical impedance tomography for measuring electrical conductivity during electroporation. Physiol Meas. 2014;35(6):985-96.

[25] Sano MB, Neal RE, Garcia PA, et al. Towards the creation of decellularized organ constructs using irreversible electroporation and active mechanical perfusion. Biomedical Engineering Online. 2010;9:83.

[26] Garcia PA, Rossmeisl JH, Neal RE, et al. Intracranial nonthermal irreversible electroporation: in vivo analysis. The Journal of Membrane Biology. 2010;236(1):127-136.

[27] Zupanic A, Kos B, Miklavcic D. Treatment planning of electroporation-based medical interventions: electrochemotherapy, gene electrotransfer and irreversible electroporation. Phys Med Biol. 2012;57(17):5425-40.

[28] Groselj A, Kos B, Cemazar M, et al. Coupling treatment planning with navigation system: a new technological approach in treatment of head and neck tumors by electrochemotherapy. Biomed Eng Online. 2015;14 Suppl 3:S2.

[29] Kos B, Voigt P, Miklavcic D, Moche M. Careful treatment planning enables safe ablation of liver tumors adjacent to major blood vessels by percutaneous irreversible electroporation (IRE). Radiol Oncol. 2015;49(3):234-41.

[30] Edhemovic I, Gadzijev EM, Brecelj E, et al. Electrochemotherapy: a new technological approach in treatment of metastases in the liver. Technol Cancer Res Treat. 2011;10(5):475-85.

[31] Khorasani, Firoozabadi SM, Shankayi Z. Finite Element Analysis of Tissue Conductivity during High-frequency and Low-voltage Irreversible Electroporation. Iranian Journal of Medical Physics. 2017;14(3):135-140.

[32] Zhao Y, Bhonsle S, Dong S, et al. Characterization of conductivity changes during high-frequency irreversible electroporation for treatment planning. IEEE Transactions on Biomedical Engineering. 2018;65(8):1810-1819.

[33] Khorasani A, Firoozabadi SM, Shankayi Z. Conductivity Changes of Liver Tissue during Irreversible Electroporation and Calculation of the Electric Field Distribution. Modares Journal of Biotechnology. 2018;9(2):227-232.

[34] Miklavčič D, Šemrov D, Mekid H, Mir LM. A validated model of in vivo electric field distribution in tissues for electrochemotherapy and for DNA electrotransfer for gene therapy. Biochimica et Biophysica Acta. 2000;1523(1):73-83.

[35] Garcia PA, Kos B, Rossmeisl Jr JH, et al. Predictive therapeutic planning for irreversible electroporation treatment of spontaneous malignant glioma. Medical Physics. 2017;44(9):4968-4980.

[36] Wagstaff PG, de Bruin DM, van den Bos W, et al. Irreversible electroporation of the porcine kidney: temperature development and distribution. Urologic Oncology. 2015;33(4):168.e1-168.e7.